Report

Cell Reports

Ubiquitylation Dynamics of the Clock Cell Proteome and TIMELESS during a Circadian Cycle

Graphical Abstract

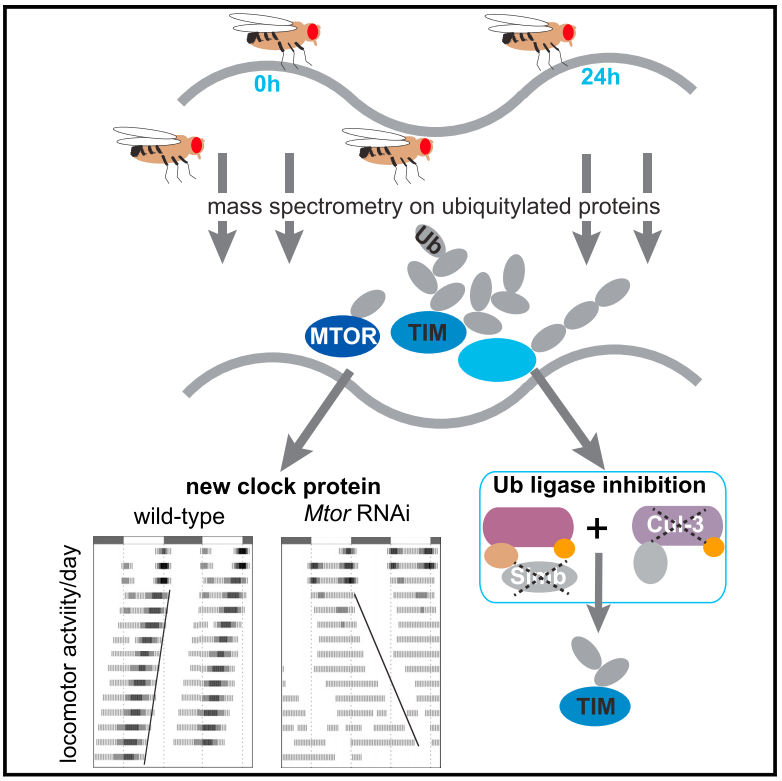

Authors

Áron Szabó, Christian Papin, David Cornu, ..., Virginie Redeker, Ugo Mayor, François Rouyer

Correspondence

aszabo0514@yahoo.com (Á.S.), rouyer@inaf.cnrs-gif.fr (F.R.)

In Brief

Rhythmic deposition of posttranslational modifications such as ubiquitin could underlie circadian rhythms. Here, Szabó et al. explore the cycling ubiquitylation landscape of the proteome in *Drosophila* and investigate the ubiquitylation of TIMELESS, a core clock protein, by its cognate ubiquitin ligases.

Highlights

- Mass spectrometry sheds light on circadian protein ubiquitylation
- MEGATOR, a chromatin-associated nucleoporin, is cyclically ubiquitylated
- MEGATOR sets the pace of the clock by regulating the core oscillator
- Ub ligase complexes of CULLIN-3 and SLIMB are redundant for TIMELESS ubiquitylation

Szabó et al., 2018, Cell Reports *23*, 2273–2282
May 22, 2018
https://doi.org/10.1016/j.celrep.2018.04.064

CellPress

Cell Reports
Report

Ubiquitylation Dynamics of the Clock Cell Proteome and TIMELESS during a Circadian Cycle

Áron Szabó,[1,6,*] Christian Papin,[1,6] David Cornu,[2] Elisabeth Chélot,[1] Zoltán Lipinszki,[3] Andor Udvardy,[3] Virginie Redeker,[1,2] Ugo Mayor,[4,5] and François Rouyer[1,7,*]
[1]Paris-Saclay Institute of Neuroscience, Université Paris-Sud, CNRS, Université Paris-Saclay, 91190 Gif-sur-Yvette, France
[2]Institute for Integrative Biology of the Cell, CEA, CNRS, Université Paris Sud, Université Paris-Saclay, 91190 Gif-sur-Yvette, France
[3]Institute of Biochemistry and MTA SZBK "Lendület" Laboratory of Cell Cycle Regulation, HAS-BRC, 6726 Szeged, Hungary
[4]Department of Biochemistry and Molecular Biology, University of the Basque Country (UPV/EHU), Leioa, Bizkaia, Spain
[5]Ikerbasque, Basque Foundation for Science, Bilbao, Bizkaia, Spain
[6]These authors contributed equally
[7]Lead Contact
*Correspondence: aszabo0514@yahoo.com (Á.S.), rouyer@inaf.cnrs-gif.fr (F.R.)
https://doi.org/10.1016/j.celrep.2018.04.064

SUMMARY

Circadian clocks have evolved as time-measuring molecular devices to help organisms adapt their physiology to daily changes in light and temperature. Transcriptional oscillations account for a large fraction of rhythmic protein abundance. However, cycling of various posttranslational modifications, such as ubiquitylation, also contributes to shape the rhythmic protein landscape. In this study, we used an *in vivo* ubiquitin labeling assay to investigate the circadian ubiquitylated proteome of *Drosophila melanogaster*. We find that cyclic ubiquitylation affects MEGATOR (MTOR), a chromatin-associated nucleoporin that, in turn, feeds back to regulate the core molecular oscillator. Furthermore, we show that the ubiquitin ligase subunits CULLIN-3 (CUL-3) and SUPERNUMERARY LIMBS (SLMB) cooperate for ubiquitylating the TIMELESS protein. These findings stress the importance of ubiquitylation pathways in the *Drosophila* circadian clock and reveal a key component of this system.

INTRODUCTION

Cycling transcripts are a key feature of circadian clock output and rely on both transcriptional and post-transcriptional mechanisms (Keegan et al., 2007; Abruzzi et al., 2011; Hughes et al., 2012; Koike et al., 2012; Kojima et al., 2012; Le Martelot et al., 2012; Menet et al., 2012; Rodriguez et al., 2013). The cycling proteome and translatome of specific tissues have, however, pointed to large differences between mRNA and protein cycling profiles (Reddy et al., 2006; Møller et al., 2007; Deery et al., 2009; Huang et al., 2013; Jouffe et al., 2013; Robles et al., 2014; Guerreiro et al., 2014; Mauvoisin et al., 2014, 2015; Neufeld-Cohen et al., 2016). For example, about 50% of rhythmic proteins in the liver cannot be accounted for by corresponding mRNA rhythms (Mauvoisin et al., 2014), indicating a major role for cycling protein synthesis or degradation (Lück et al., 2014). Extensive circadian post-translational modifications such as acetylation (Masri et al., 2013) and phosphorylation (Robles et al., 2017; Wang et al., 2017) have been observed in the liver. However, little is known about the circadian control of ubiquitylation, which is the main protein degradation signal (Clague and Urbé, 2010; Kleiger and Mayor, 2014). This even holds for core clock proteins, whose oscillations depend on several ubiquitin (Ub) ligases and proteases (Chiu et al., 2011; Grima et al., 2012; Luo et al., 2012; Hirano et al., 2013, 2016; Yoo et al., 2013; Stojkovic et al., 2014). We therefore set out to understand how the *Drosophila* clock might govern daily rhythms in ubiquitylation by searching for circadian oscillations in the amount of ubiquitylated proteins.

RESULTS AND DISCUSSION

Characterization of the Circadian Ubiquitylated Proteome

We took advantage of the biotinylated Ub (bioUb) system to analyze the circadian control of protein ubiquitylation in clock-containing cells of the *Drosophila* head. bioUb allows Ub purification based on BirA-mediated *in vivo* biotinylation of Ub fused to AviTag (Franco et al., 2011; Martinez et al., 2017; Pirone et al., 2017). First, we asked whether overexpression of tagged Ub would perturb endogenous timekeeping. When we expressed a GAL4-inducible transgene that encoded biotinylatable Ub (upstream activating sequence [*UAS*]-*(bioUb)$_6$-birA*) or the control *UAS-birA* with the clock cell-specific driver *tim-gal4*, only one insertion of the *UAS-(bioUb)$_6$-birA* transgene lengthened the period of sleep-wake cycles, measured as daily changes in locomotor activity (Table S1, bioUb insertion on chromosome II). At the molecular level, TIMELESS (TIM) and PERIOD (PER) oscillations on western blots of head extracts of *w; tim-gal4/+* and *w; tim-gal4, UAS-(bioUb)$_6$-birA/+* (*tim>bioUb*) flies were very similar (Figure 1A). Clock proteins in head extracts mainly derive from the retina, which houses its own clock, whereas locomotor activity rhythms in constant darkness largely depend on the small lateral ventral neuron (sLNv) oscillator of the brain clock network. Different effects of bioUb expression may thus occur because of the different cell types. For example, Ub overexpression could slightly affect clock protein accumulation or modify cell physiology to produce sLNv-specific period

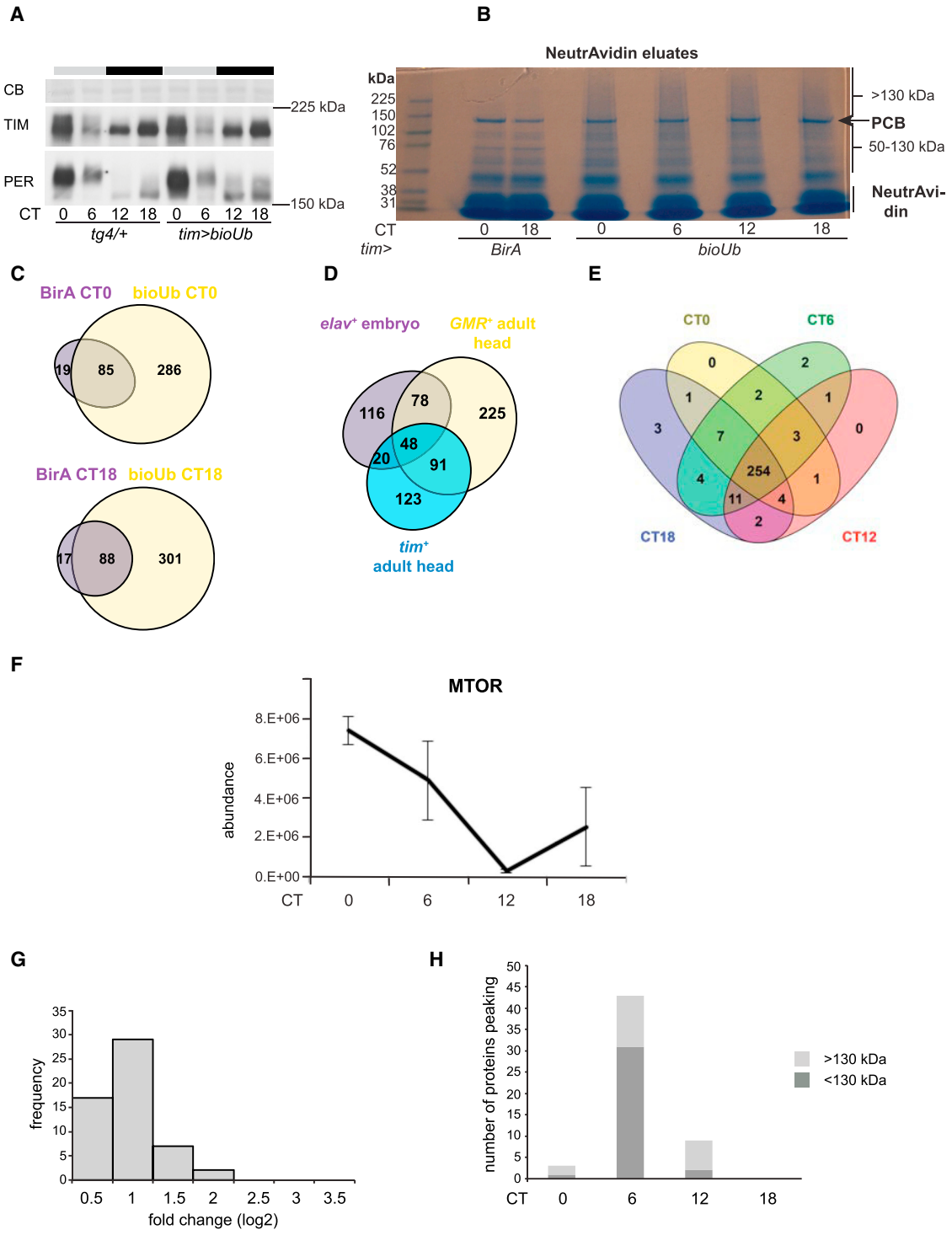

Figure 1. Identification of the Rhythmic Ubiquitylated Proteome

CT means circadian time. Gray and black bars represent subjective day and subjective night, respectively.

(A) PER and TIM western blots (WBs) of *w; tim-gal4/+* (*tg4/+*) and *w; tim-gal4, UAS-(bioUb)$_6$-birA/+* (*tim>bioUb*) head extracts. CB denotes a Coomassie-stained band as a loading control. Two independent experiments were done.

(B) Coomassie-stained PAGE gel of ubiquitylated proteins from *w; tim-gal4, UAS-(bioUb)$_6$-birA/+* (*bioUb*) and *w; tim-gal4, UAS-birA/+* (*BirA*) control flies. Left: protein markers (in kilodaltons). The PCB band itself was not excised. NeutrAvidin contaminates the 15- to 30-kDa region. The gel is representative of three independent experiments.

(legend continued on next page)

changes. Nevertheless, the bioUb system can be applied to clock studies with minimal perturbation of the timekeeping mechanism, at least in the retina. To capture the ubiquitylated proteome, *tim>bioUb* and *w; tim-gal4, UAS-birA/+* (*tim>birA*) control flies were entrained to 12 hr:12 hr light-dark (LD) cycles and were collected on the first day of constant darkness (DD1). NeutrAvidin-bound fractions of head lysates were separated by SDS-PAGE (Figure 1B). Two gel regions (50–130 kDa and >130 kDa) were selected to avoid inclusion of the 130-kDa band corresponding to the abundant, endogenously biotinylated PYRUVATE CARBOXYLASE (PCB) protein (Tong, 2013). Proteins of three replicates were in-gel digested with trypsin and subsequently identified and quantified using nano-liquid chromatography-tandem mass spectrometry and label-free quantification (Schilling et al., 2012).

Approximately 300 different proteins were identified exclusively in bioUb-purified eluates at each of two time points where BirA-only controls were available (Figure 1C). We compared the ubiquitylome of *tim*$^+$ clock cells with two recent datasets from embryonic neuronal cells and adult photoreceptors (Ramirez et al., 2015). 91 ubiquitylated proteins were found in both photoreceptors and clock cells, whereas 123 proteins were identified in clock cells only (Figure 1D; Table S2), providing a proxy to identify the clock cell-specific proteome in flies. Notably, ubiquitylated TIM and the clock kinase SHAGGY (SGG) were only found in *tim*$^+$ cells as well as four subunits of the proteasome regulatory complex. Quantitative intensities in replicates displayed strong reproducibility (Figure S1A; Supplemental Experimental Procedures). 344 proteins were significantly more abundant at circadian time (CT) 0 (beginning of the subjective day on DD1) in the bioUb samples compared with the BirA control ($p < 0.05$, fold change >2) (Figures S1B and S2C). Pairwise comparison of bioUb time points resulted in the identification of several differentially represented bioUb-ylated proteins ($p < 0.05$) (Figure 1E). Ubiquitylated proteins were found to be enriched at CT6 relative to other times (Figure S1D). Subsequently, the fitting of changes in protein abundance to theoretical cosine curves (adapted from Robles et al., 2014) was evaluated at four phases 6 hr apart. Oscillation in abundance was observed for 52 proteins (15% of all bioUb-ylated proteins) (Table S3) when using cutoffs of "distance" <0.15 for curve fitting and $p < 0.2$ for opposing time points (Supplemental Experimental Procedures). Megator (MTOR), a nuclear pore complex (NPC) component (Zimowska et al., 1997), stood out, showing robust cycling with very high (29-fold) peak-to-peak amplitude (Figure 1F). Generally, fold changes in abundance of ubiquitylated proteins were centered below 2 (Figure 1G), which is similar to the circadian cycling of total protein levels in the mammalian liver (Mauvoisin et al., 2014; Robles et al., 2014). Oscillations of all 52 candidates were manually checked. We observed a non-uniform phase distribution of ubiquitylated proteins (Figure S1D; Table S3); most peaked at CT6 (n = 43), followed by CT12 (n = 9) (Figure 1H). We conclude that protein ubiquitylation in clock cells is concentrated around daytime hours. In contrast, circadian-controlled protein synthesis is positioned mostly at CT7 (noon) and CT19 (midnight) in a bimodal fashion (Huang et al., 2013). Interestingly, three proteins (ARR1, NMDMC, and HN) showed cycling in both SDS-PAGE gel regions (50–130 kDa and >130 kDa) (Table S3), suggesting that highly ubiquitylated forms of these low-molecular-weight (33–52 kDa) proteins are also rhythmically regulated. The cycling pool of 52 ubiquitylated proteins was enriched for neuronal and memory proteins versus all ubiquitylated entries (Figure S2A). Gene Ontology (GO) terms for the proteasome regulatory particle subunits and synaptic proteins were also more represented in the cycling ubiquitylome than in the total *tim*$^+$ cell translatome (Huang et al., 2013; Figure S2B).

Subsequently, we compared the cycling translatome (Huang et al., 2013) and the cycling ubiquitylome of *tim+* cells. Only three proteins showed both rhythmic translation and ubiquitylation: W (a transporter for eye pigment precursors), PVR (a receptor tyrosine kinase), and RAB32/LTD (a synaptic Rab GTPase). Their translation phases (maximum at CT21, CT14, and CT17, respectively) appeared offset from their ubiquitylation phases (maximum at CT6 in all cases). The delay between peak translation and ubiquitylation suggested a rather long half-life for these rhythmically translated proteins. 10 of the cycling candidates also showed significant ($p < 0.05$) abundance changes between opposing phases (Table S4; Figure S2C).

MTOR Is Cyclically Ubiquitylated and Affects the Core Pacemaker

To verify the oscillations that were identified by mass spectrometry, we tested seven proteins by western blotting (HSP83, AP-2α, ARI-1, INX3, MTOR, and SGG) based on the strength of their oscillations (low distance value [<0.055] or significant amplitude [$p < 0.05$]; Table S3) and availability of specific antibodies. Four (HSP83, NRV2, MTOR, and SGG) showed recognizable ubiquitylation on immunoblots of purified bioUb extracts (Figure 2A; Figures S3A and S3C). NRV2, despite being ubiquitylated, did not show cycling ubiquitylated states (Figures S3A and S3B). The ubiquitylated form of the SGG46 isoform of the SGG kinase (Ruel et al., 1993; Martinek et al., 2001) and the HSP83 chaperone demonstrated dispersed phases of oscillation among replicates, although a clear cycling was observed in each time series of samples (Figures S3A, S3C, and S3F). These proteins did not significantly cycle in head extracts (Figures S3B and S3D) and neither did total levels of ubiquitylated proteins in the same material (Figure S3E). In contrast, anti-MTOR immunoblotting

(C) Venn diagrams showing the number of proteins identified in bioUb versus control (BirA) pull-down at CT0 and CT18.
(D) Comparison of proteins found in previous bioUb purifications from *elav-gal4*-expressing embryonic (*elav*$^+$ *embryo*) and *GMR-gal4*-expressing adult eye (*GMR*$^+$ *adult head*) neurons (Ramirez et al., 2015) with our dataset (*tim*$^+$ *adult head*). Numbers correspond to protein species.
(E) Venn diagram of protein species found in bioUb eluates and not in control purifications at the four time points.
(F) Average abundance profile (with SD) of MTOR.
(G) 83% of cycling ubiquitylated proteins change in abundance less than 2-fold across the cycle (1.7 on average).
(H) Number of oscillating ubiquitylated proteins showing maximum abundance at the indicated phase. Ubiquitylation peaks at CT6 for 78% of proteins.
See also Figures S1 and S2.

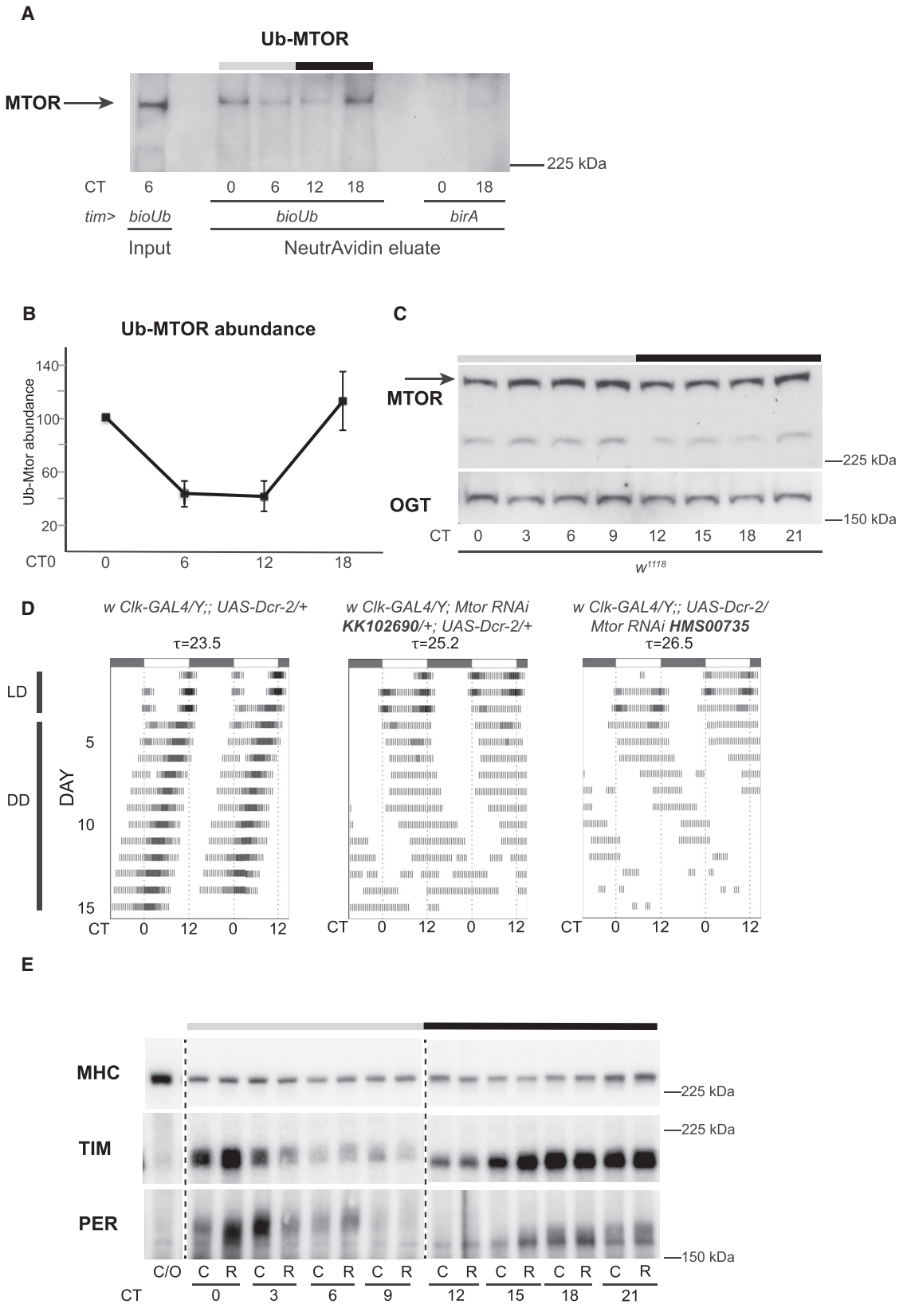

(legend on next page)

unequivocally confirmed an oscillation of ubiquitylation in purified bioUb samples (Figures 2A and 2B). To control for a possible rhythmicity in total protein levels, we blotted head lysates with anti-MTOR. Protein levels did not cycle (Figures 2C, S3G, and S3H), indicating that cycling ubiquitylation of this protein is not a mere consequence of rhythmic total protein levels. MTOR is the innermost nucleoporin forming the nuclear basket with NUP153 (Zimowska et al., 1997). It is involved in the control of cell division (Zimowska et al., 1997; Qi et al., 2004; Liu et al., 2015) and has additional roles in chromatin modulation (Mendjan et al., 2006; Lagarou et al., 2008; Vaquerizas et al., 2010).

To gauge whether MTOR feeds back onto the core molecular oscillator, we used clock cell Gal4 drivers to express two UAS-RNAi insertions targeting distinct regions of *Mtor*. Both caused behavioral period lengthening and decreased the amplitude of rhythmicity (Figure 2D; Table S1). To rule out gross neuronal morphology defects as a cause of the behavioral phenotype, we stained key pacemaker neurons, sLNvs, for the neuropeptide pigment dispersing factor (PDF). PDF-expressing cells showed normal projections (Figure S3I). Western blots of head extracts from *Mtor* RNAi flies showed strongly reduced MTOR levels (Figure S3J) and uncovered increased PER and TIM levels at daybreak (CT0) (Figure 2E), in agreement with the lengthening of the behavioral period. The observed lag in PER and TIM disappearance on western blots in the morning is likely to induce a sustained transcriptional repression by PER, explaining the long behavioral period of *Mtor* RNAi flies.

The function of MTOR as a nucleoporin prompted us to investigate the subcellular localization of PER, TIM, and CLK in the sLNvs of *Mtor* RNAi flies. We stained for these proteins at times when PER and TIM are predominantly nuclear in wild-type animals, at CT24 (beginning of day 2 of DD) and CT45 (end of day 2) in control (*w; UAS-Dcr-2/+; gal1118/+*) and experimental *Mtor* RNAi knockdown (*w; UAS-Dcr-2/+; gal1118/ Mtor* RNAi) flies. PER and TIM normally undergo finely regulated cytoplasmic-to-nuclear transition from CT18 onward to fulfill their roles as transcriptional repressors. TIM and PER showed a more cytoplasmic localization at both time points in *Mtor* RNAi sLNvs (Figures S4A–S4D) compared with the wild-type, suggesting that defective nuclear localization of these proteins could contribute to the behavioral period lengthening (0.9 hr in this genotype; Table S1). The nuclear localization defect of the clock proteins in *Mtor* RNAi flies might thus be involved in the broadening of the PER/TIM peak and hence contribute to the lengthening of the behavioral period. Nup153, another basket nucleoporin, was recently shown to be involved in the control of PER/TIM nuclear translocation (Jang et al., 2015).

CUL-3 and SCF^{SLMB} Play a Partly Redundant Role in the Rhythmic Ubiquitylation of TIM

We noticed that TIM was detected with two peptides specific to the bioUb-purified mass spectrometry samples only at CT18. Although quantification of peptide intensities did not show a significant oscillation in TIM levels, we endeavored to analyze the temporal dynamics of TIM ubiquitylation. We observed slowly migrating TIM bands in *tim>bioUb* pull-downs (Figure 3A). The bulk of the TIM signal in NeutrAvidin eluates was concentrated around the highest phosphorylated forms of non-ubiquitylated TIM in the input. A roughly 10-kDa difference between the lowest bands in the input and pull-down strongly suggested that TIM is modified by at least one Ub moiety at all circadian times. In the late night and morning, putative polyubiquitylated TIM (Ub-TIM) species were observed. Although Ub-TIM quantity appeared to cycle with a peak at CT15–CT21 (Figure 3A), TIM was found to be substantially more ubiquitylated at CT0, CT3, and CT6 after normalization to total TIM levels (Figure 3B). This enrichment in TIM ubiquitylation temporally correlated with the strong decrease in TIM levels that occurs at the night/day transition, supporting that TIM ubiquitylation cycling drives its proteasomal degradation.

To independently validate the results obtained with bioUb pull-down of TIM, we explored other Ub purification possibilities. *In vivo* expression of tagged cognate Ub receptors showing affinity to ubiquitylated TIM forms could also allow the isolation of Ub-TIM by tag-specific affinity chromatography (Low et al., 2013). Knockdown of known polyubiquitin receptors (Table S1) revealed that all of them participated in the circadian control of activity rhythms. Adult-restricted downregulation of the extra-proteasomal polyubiquitin receptor *Dsk2*/*Ubiquilin* (*Ubqn*) increased TIM levels during the daytime and early evening, suggesting that it was involved in TIM degradation (Figure 3C). We thus used FLAG-Dsk2 to pull down Ub-TIM. Head extracts from flies expressing FLAG-Dsk2 only in *tim*$^{+}$ cells were prepared under mild conditions to preserve the Dsk2-Ub-TIM interaction. TIM co-precipitated with FLAG-Dsk2 and showed daily cycling (Figures 3D and 3E), in agreement with the Ub-TIM oscillations in bioUb precipitates. Expression of a tagged version of the proteasomal Ub receptor p54/Rpn10 and subsequent pull-down also resulted in purification of Ub-TIM in the morning (Figure 3F).

Substrates of Ub ligases can be modified by Ub in various forms. Besides the addition of a single Ub moiety to the target lysine, the attached Ub can be further polyubiquitylated on its internal lysines (for example K48, K11, or K63), resulting in Ub chains or on its N-terminal methionine, which yields a linear chain

Figure 2. Rhythmic Ubiquitylation of MTOR Unveils a Core Clock Component

Three independent experiments were performed for each blot.

(A) MTOR WB of *tim > bioUb and tim > birA* NeutrAvidin-purified samples. Input of *tim>bioUb* is shown on the left. Equal binding and elution in each sample were confirmed by mass spectrometry quantification of eluted ubiquitin (see Figure S1D for an example).

(B) Ubiquitylated MTOR was quantified in *tim>bioUb* pull-downs (n = 3). Error bars represent SEM. Values at CT0 were scaled to 100.

(C) MTOR WB of *w*^{1118} flies with O-glycosyl transferase (OGT) as loading control. The arrow indicates MTOR.

(D) Double-plotted averaged actograms of control and two different *Mtor* RNAi-expressing genotypes. τ indicates the period (hours).

(E) PER and TIM WB of *w Clk-GAL4/Y;; UAS-Dcr-2/+* (C) and *w Clk-GAL4/Y;; UAS-Dcr-2/Mtor RNAi HMS00735* (R) with myosin heavy chain (MHC) as a loading control. *Clk*^{out} (C/O) served as negative control for PER and TIM immunoreactivity.

See also Figures S3 and S4.

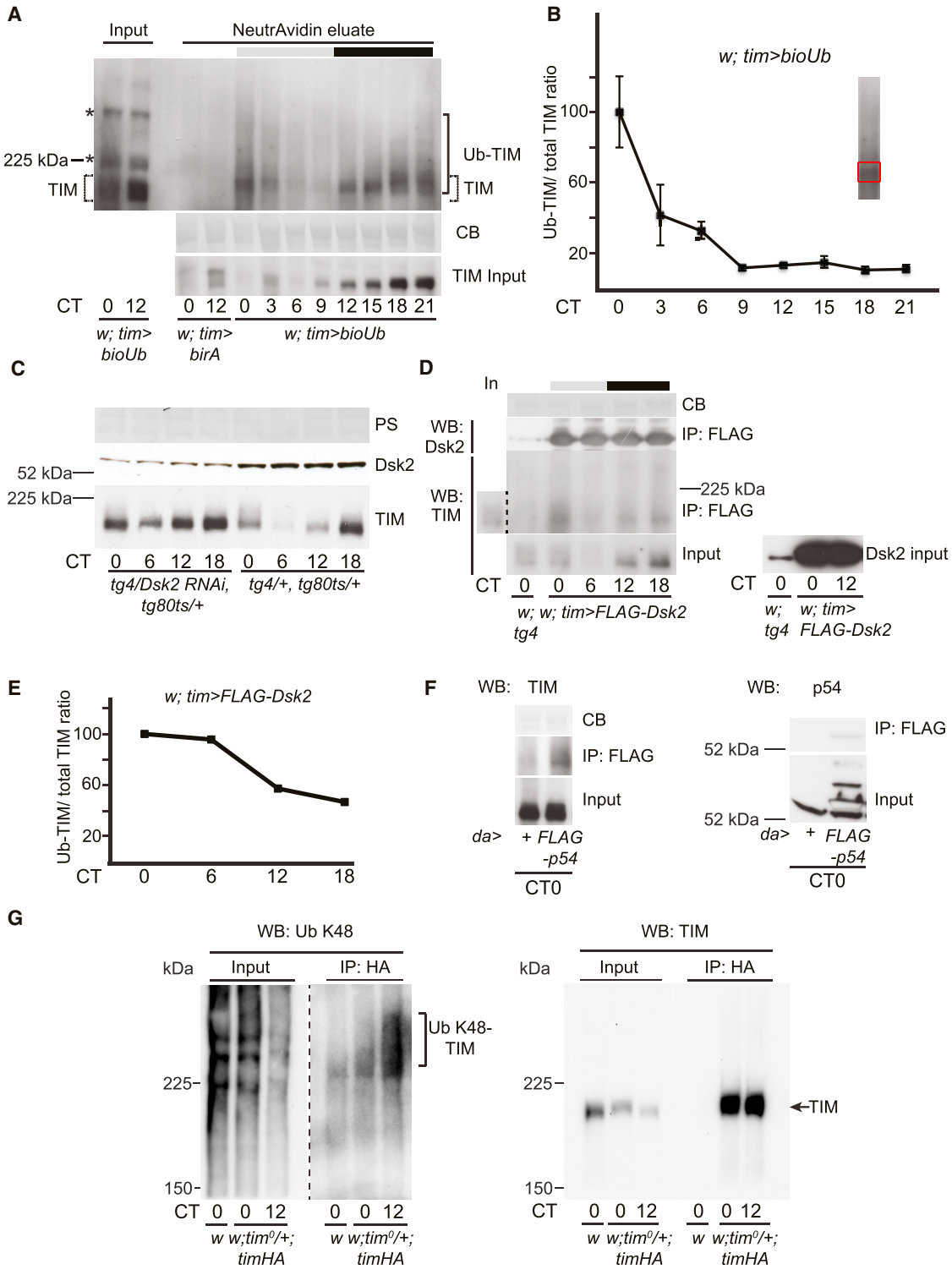

Figure 3. Cyclic TIM Ubiquitylation Can Be Revealed by bioUb Purification, Ub Receptor Pull-Down and Ub Chain-Specific Antibodies

At least two independent experiments were performed for each blot.

(A) TIM WB of NeutrAvidin-purified samples from *tim > bioUb and tim > birA* flies. Inputs are shown below as well as on the same gel for two time points. Ub-TIM means ubiquitylated TIM. Asterisks mark non-specific bands in the input.

(B) Ubiquitylated TIM (framed in the inset) was quantified and normalized to total TIM (input). Error bars represent deviation from the mean (n = 2). The mean ratio at CT0 was scaled to 100.

(legend continued on next page)

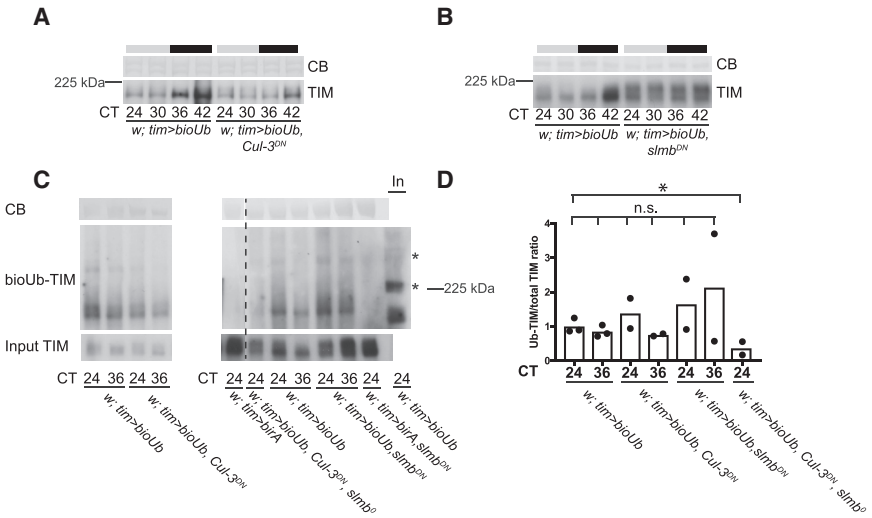

Figure 4. Deciphering the Roles of Cognate Ubiquitin Ligases of TIM in TIM Ubiquitylation

At least two independent experiments were performed for each blot.

(A and B) Head extracts of flies with (A) Cul-3 or (B) Slmb inhibition were blotted for TIM.

(C) TIM WBs of NeutrAvidin-purified samples from various ubiquitin ligase mutants in a bioUb background (see full genotypes in the Experimental Procedures). Input was also loaded next to the purified material (In). Asterisks marks non-specific bands in the input. *w; tim > bioUb, Cul-3^{DN}* samples and their controls were run on a separate gel.

(D) Ubiquitylated TIM was quantified and normalized to total TIM (input). The ratio in *tim>bioUb* at CT24 was set to 1. Circles indicate individual data points. Paired two-tailed t test was used for statistics. *p = 0.0143; n.s., not significant.

conformation (Kwon and Ciechanover, 2017). To decipher the Ub code on TIM, we immunoprecipitated hemagglutinin (HA)-tagged TIM from *w; tim^{0}/+; timHA* flies and revealed Ub chain types by western blotting with Ub linkage type-specific antibodies. K48-linked polyubiquitylation is a classical proteasomal degradation signal. Intriguingly, we found K48-linked polyubiquitylation on TIM only at CT12 (evening), when freshly synthesized TIM is presumed to undergo heavy degradation to delay protein accumulation as opposed to the peak production of the *tim* mRNA (Figure 3G). The hypo-phosphorylated TIM that is present at this time is preferentially bound by CUL-3 Ub ligase complexes (Grima et al., 2012). Taken together, combined data from three approaches strongly support an oscillation of TIM ubiquitylation during a circadian cycle.

A number of Ub ligases (Grima et al., 2002, 2012; Ko et al., 2002; Koh et al., 2006; Peschel et al., 2006, 2009; Knowles et al., 2009; Lamaze et al., 2011; Ozturk et al., 2013; Guo et al., 2014) and proteases (Luo et al., 2012) are implicated in the *Drosophila* circadian oscillator and its synchronization by light. However, actual ubiquitylation of TIM has only been reported by the SCF^{JETLAG} E3 ligase as a consequence of a light pulse (Naidoo et al., 1999; Koh et al., 2006). SCF^{SLMB} and CUL-3 Ub ligases were found to control TIM oscillations in constant darkness (Grima et al., 2002, 2012). Therefore, we aimed to distinguish the contributions of SLMB and CUL-3 to the ubiquitylation state of TIM *in vivo*. Expression of dominant-negative forms of SLMB (*UAS-slmb$^{\Delta F}$*) and CUL-3 (*UAS-Cul-3^{K717R}*) on the bioUb background led to behavioral arrhythmicity of flies (Table S1; Ko et al., 2002; Grima et al., 2012). Phosphorylated TIM accumulated in *Cul-3^{K717R}* flies (Figure 4A), as reported previously (Grima et al., 2012), whereas *slmb$^{\Delta F}$* flies showed accumulation of hyperphosphorylated TIM (Figure 4B), similar to *slmb^{0}* mutants (Grima et al., 2002, 2012). Ubiquitylated TIM did not decrease in *Cul-3^{K717R}* flies, indicating that CUL-3 inhibition does not induce changes in TIM ubiquitylation levels (Figures 4C and 4D). In *slmb$^{\Delta F}$* flies, we observed an increase of ubiquitylated TIM that mostly reflected increased TIM levels (Figures 4C and 4D). However, the inhibition of both enzymatic activities in *slmb^{0} Cul-3^{K717R}* flies led to reduced ubiquitylated TIM levels, indicating that CUL-3 and SCF^{SLMB} are the main E3 ligases for the circadian control of TIM ubiquitylation and play at least a partly redundant or cooperative role in the ubiquitylation of TIM sites (Figures 4C and 4D). Interestingly, SCF^{SLMB} mainly assembles K11-based Ub chains on CUBITUS INTERRUPTUS, whereas CUL-3^{Rdx} prefers building K48-linked chains on the same protein (Zhang et al., 2013). It is tempting to speculate that TIM is subject to the same modifications by the SCF^{SLMB} and CUL-3 Ub ligase complexes, with one partially substituting for the other. Further investigations are required to elucidate the chain-building specificities of SCF^{SLMB} and CUL-3 on TIM; nonetheless, we demonstrated the presence of K48-linked Ub chains on TIM specifically in the evening.

In this study, we describe a layer of circadian output organization in the form of rhythmic ubiquitylation with a peak of proteome ubiquitylation around CT6. In the mammalian liver, the phase distribution of cycling proteins shows a peak around

(C) TIM and Dsk2 WBs of *w; tim-gal4/+; tubulin-gal80^{ts}/+* (*tg4/+, tg80ts/+*) and *w; tim-gal4/UAS-Dsk2 RNAi 16/1; tubulin-gal80^{ts}/+* (*tg4/Dsk2 RNAi, tg80ts/+*). Flies were grown at 18°C to repress Gal4 with Gal80^{ts}, and emerged adults were transferred at 29°C for analysis at DD1 after LD entrainment. PS means Ponceau S staining.

(D) TIM and Dsk2 WBs of *w; tim-gal4/+* (*w; tg4*) and *tim>FLAG-Dsk2* anti-FLAG precipitates. A *tim>FLAG-Dsk2* CT0 input (In) is loaded next to the precipitates. 20 μg of input were blotted for TIM (input) and Dsk2 (Dsk2 input).

(E) Ubiquitylated TIM was quantified and normalized to total TIM (input). The ratio at CT0 was set to 100.

(F) TIM and p54 WBs of *w;;daughterless (da)-gal4* (+) and *da>FLAG-p54* (*FLAG-p54*) anti-FLAG precipitates.

(G) Anti-HA immunoprecipitates of *w* and *w;tim^{0}/+;timHA* extracts were blotted for TIM and for K48-linked Ub chains. Note that, for anti-Ub K48, a lower exposition image of the input is shown compared with the precipitate lanes for easier discrimination of individual ubiquitylated bands.

CT20 (Reddy et al., 2006; Lück et al., 2014; Mauvoisin et al., 2014; Robles et al., 2014), whereas one-third of Ub ligase mRNAs peak around CT6 (Hughes et al., 2009). These putatively antiphasic oscillations between synthesis and degradation are predicted to promote strong oscillations (Lück et al., 2014). A proteome-wide analysis of circadian protein cycling is currently missing in flies, but our results with TIM reveal a large phase delay between the peak of TIM levels (CT18) and TIM bulk ubiquitylation (CT0). However, K48-linked ubiquitylation, a major degradation signal, rather peaks at CT12 on TIM, according to our results, possibly preventing TIM from accumulating synchronously with its mRNA, which peaks at CT12. The Ub chain type that drives quantitative elimination of TIM in the morning remains enigmatic, but the K11 linkage type could contribute (Kwon and Ciechanover, 2017). Using a proteomics approach, we identified 52 rhythmically ubiquitylated proteins. The notion of circadian control of these oscillations is reinforced by differential TIM ubiquitylation in DD2 that is approximately in sync with TIM ubiquitylation patterns throughout DD1 (Figures 3A and 4C).

In addition to controlling rhythmic protein degradation, circadian regulated ubiquitylation is likely to direct oscillations of protein function, as exemplified by the robust rhythmic ubiquitylation of MTOR. Constant steady-state levels of MTOR make it improbable that its cycling low-level ubiquitylation would target it for degradation. Our data thus suggest that its nucleoporin or chromatin regulator activity is circadian controlled, and it will be interesting to see whether it contributes to the circadian modulation of the nuclear protein accumulation, which concerns 13% of the liver proteome in mammals (Wang et al., 2017).

EXPERIMENTAL PROCEDURES

Further details and an outline of resources used in this work can be found in the Supplemental Experimental Procedures.

Experimental Model and Subject Details

Adult *Drosophila melanogaster* were used throughout this study. Flies were 1–4 days old at the start of experiments. Stocks were maintained on a 12 hr:12 hr LD cycle on standard corn meal-yeast-agar medium at 25°C. *w; tim-gal4, UAS-(bioUb)$_6$-birA/+*, *w; tim-gal4, UAS-birA/+*, and *w;; UAS-FLAG-Cul-3^{K717R}*, *slmb8, hs-slmb* were created by standard meiotic recombination. *slmb0 (slmb8 hs-slmb)* adults were produced by providing *HS-SLMB* expression with daily heat shocks (1 hr 15 min, 37°C) during development, as described by Grima et al. (2002). Flies were entrained to 4 complete LD cycles at 25°C and collected on DD1 unless stated otherwise.

Genotypes commonly used in this study were as follows:

w; tim-gal4, UAS-birA/+ (*w; tim > birA*)
w; tim-gal4, UAS-(bioUb)$_6$-birA/+ (*w; tim > bioUb*)
w; tim-gal4, UAS-birA; UAS-FLAG-Cul-3^{K717R} (*w; tim > birA, Cul-3^{DN}*)
w; tim-gal4, UAS-(bioUb)$_6$-birA/tim-gal4; UAS-FLAG-Cul-3^{K717R} (*w; tim > bioUb, Cul-3^{DN}*)
w; tim-gal4, UAS-birA; UAS-slmb$^{\Delta F}$ (*w; tim > birA, slmb^{DN}*)
w; tim-gal4, UAS-(bioUb)$_6$-birA/tim-gal4; UAS-slmb$^{\Delta F}$ (*w; tim > bioUb, slmb^{DN}*)
w; tim-gal4, UAS-(bioUb)$_6$-birA/tim-gal4; UAS-FLAG-Cul-3^{K717R}, slmb8, hs-slmb (w; tim > bioUb, Cul-3^{DN}, slmb^{0}).

Quantification and Statistical Analysis

All statistical analyses for mass spectrometry were done on biological triplicates with the Perseus 1.5.1.6 software (Max Planck Institute of Biochemistry). A p value of 0.2 from Welch's t test between time points (CT6 versus CT18 or CT0 versus CT12 depending on the phase) was used as cutoff for significance of the peak-to-peak amplitude.

Error bars in other experiments represent SD unless stated otherwise (defined in the figure legends). For comparison of protein abundances in Figure 4D, we used paired two-tailed t tests. For experiments on nucleocytoplasmic clock protein localization (Figure S4), we first tested for normal distribution of intensity values under each condition with the D'Agostino-Pearson normality test. In case of normal distribution, Welch's unpaired two-tailed t test was applied for pairwise comparison between wild-type and *Mtor* RNAi conditions. In the absence of normal distribution, we used the Mann-Whitney test. The significance threshold in each case was established as $p < 0.05$. Calculations were done, and the graphs in Figure 4D were created in Prism 7.0c (GraphPad).

DATA AND SOFTWARE AVAILABILITY

The accession numbers for the mass spectrometry proteomics data reported in this paper are ProteomeXchange Consortium: PXD005015 and 10.6019/PXD005015.

SUPPLEMENTAL INFORMATION

Supplemental Information includes Supplemental Experimental Procedures, four figures, and four tables and can be found with this article online at https://doi.org/10.1016/j.celrep.2018.04.064.

ACKNOWLEDGMENTS

We thank A. Chatterjee and S. Andreazza for helping with the fly work, B. Grima for sharing results about other Ub purification methods, and M. Boudinot for the FaasX software. We also thank J. Jiang for the *slmb^{DN}* stock, C.T. Chien for *cul-3* stocks, N. Glossop for *Clk-GAL4* lines, and F.R. Jackson for unpublished datasets on the translatome of *tim^{+}* cells. We are very grateful to Mads Gyrd-Hansen for the Ub chain type antibodies; C.P. Verrijzer for the MTOR antibody; and R. Paro, N. Gay, G. Beitel, A. Ferrus, J. Mueller, F. Peronnet, and R. Bauer for other antibodies. This study was supported by the following grants: DrosoClock, ClockGene, and FunGenDroso (ANR); Equipe FRM (FRM) and EUCLOCK and INsecTIME (EU 6th and 7th Framework Programs) to F.R. and GINOP-2.3.2-15-2016-00001 (Ministry for National Economy of Hungary) and OTKA-PD115404 (National Research, Development and Innovation Office) to Z.L. U.M. is a recipient of MINECO grant SAF2013-44782-P (co-financed by FEDER funds). F.R. and V.R. are supported by INSERM.

AUTHOR CONTRIBUTIONS

A.S., F.R., D.C., and V.R. conceived the experiments. A.S., C.P., E.C., and D.C. conducted the experiments. Z.L., A.U., and U.M. provided fly stocks, antibodies, datasets, and useful comments. A.S., D.C., V.R., and F.R. wrote the manuscript.

DECLARATION OF INTERESTS

The authors declare no competing interests.

Received: July 10, 2017
Revised: February 10, 2018
Accepted: April 13, 2018
Published: May 22, 2018

REFERENCES

Abruzzi, K.C., Rodriguez, J., Menet, J.S., Desrochers, J., Zadina, A., Luo, W., Tkachev, S., and Rosbash, M. (2011). Drosophila CLOCK target gene characterization: implications for circadian tissue-specific gene expression. Genes Dev. *25*, 2374–2386.

Chiu, J.C., Ko, H.W., and Edery, I. (2011). NEMO/NLK phosphorylates PERIOD to initiate a time-delay phosphorylation circuit that sets circadian clock speed. Cell *145*, 357–370.

Clague, M.J., and Urbé, S. (2010). Ubiquitin: same molecule, different degradation pathways. Cell *143*, 682–685.

Deery, M.J., Maywood, E.S., Chesham, J.E., Sládek, M., Karp, N.A., Green, E.W., Charles, P.D., Reddy, A.B., Kyriacou, C.P., Lilley, K.S., and Hastings, M.H. (2009). Proteomic analysis reveals the role of synaptic vesicle cycling in sustaining the suprachiasmatic circadian clock. Curr. Biol. *19*, 2031–2036.

Franco, M., Seyfried, N.T., Brand, A.H., Peng, J., and Mayor, U. (2011). A Novel Strategy to Isolate Ubiquitin Conjugates Reveals Wide Role for Ubiquitination during Neural Development. Mol. Cell Proteomics *10*, M110.002188.

Grima, B., Lamouroux, A., Chélot, E., Papin, C., Limbourg-Bouchon, B., and Rouyer, F. (2002). The F-box protein slimb controls the levels of clock proteins period and timeless. Nature *420*, 178–182.

Grima, B., Dognon, A., Lamouroux, A., Chélot, E., and Rouyer, F. (2012). CULLIN-3 controls TIMELESS oscillations in the Drosophila circadian clock. PLoS Biol. *10*, e1001367.

Guerreiro, A.C., Benevento, M., Lehmann, R., van Breukelen, B., Post, H., Giansanti, P., Maarten Altelaar, A.F., Axmann, I.M., and Heck, A.J. (2014). Daily rhythms in the cyanobacterium synechococcus elongatus probed by high-resolution mass spectrometry-based proteomics reveals a small defined set of cyclic proteins. Mol. Cell. Proteomics *13*, 2042–2055.

Guo, F., Cerullo, I., Chen, X., and Rosbash, M. (2014). PDF neuron firing phase-shifts key circadian activity neurons in Drosophila. eLife *3*, e02780.

Hirano, A., Yumimoto, K., Tsunematsu, R., Matsumoto, M., Oyama, M., Kozuka-Hata, H., Nakagawa, T., Lanjakornsiripan, D., Nakayama, K.I., and Fukada, Y. (2013). FBXL21 regulates oscillation of the circadian clock through ubiquitination and stabilization of cryptochromes. Cell *152*, 1106–1118.

Hirano, A., Fu, Y.H., and Ptáček, L.J. (2016). The intricate dance of post-translational modifications in the rhythm of life. Nat. Struct. Mol. Biol. *23*, 1053–1060.

Huang, Y., Ainsley, J.A., Reijmers, L.G., and Jackson, F.R. (2013). Translational profiling of clock cells reveals circadianly synchronized protein synthesis. PLoS Biol. *11*, e1001703.

Hughes, M.E., DiTacchio, L., Hayes, K.R., Vollmers, C., Pulivarthy, S., Baggs, J.E., Panda, S., and Hogenesch, J.B. (2009). Harmonics of circadian gene transcription in mammals. PLoS Genet. *5*, e1000442.

Hughes, M.E., Grant, G.R., Paquin, C., Qian, J., and Nitabach, M.N. (2012). Deep sequencing the circadian and diurnal transcriptome of Drosophila brain. Genome Res. *22*, 1266–1281.

Jang, A.R., Moravcevic, K., Saez, L., Young, M.W., and Sehgal, A. (2015). Drosophila TIM binds importin α1, and acts as an adapter to transport PER to the nucleus. PLoS Genet. *11*, e1004974.

Jouffe, C., Cretenet, G., Symul, L., Martin, E., Atger, F., Naef, F., and Gachon, F. (2013). The circadian clock coordinates ribosome biogenesis. PLoS Biol. *11*, e1001455.

Keegan, K.P., Pradhan, S., Wang, J.P., and Allada, R. (2007). Meta-analysis of Drosophila circadian microarray studies identifies a novel set of rhythmically expressed genes. PLoS Comput. Biol. *3*, e208.

Kleiger, G., and Mayor, T. (2014). Perilous journey: a tour of the ubiquitin-proteasome system. Trends Cell Biol. *24*, 352–359.

Knowles, A., Koh, K., Wu, J.T., Chien, C.T., Chamovitz, D.A., and Blau, J. (2009). The COP9 signalosome is required for light-dependent timeless degradation and Drosophila clock resetting. J. Neurosci. *29*, 1152–1162.

Ko, H.W., Jiang, J., and Edery, I. (2002). Role for Slimb in the degradation of Drosophila Period protein phosphorylated by Doubletime. Nature *420*, 673–678.

Koh, K., Zheng, X., and Sehgal, A. (2006). JETLAG resets the Drosophila circadian clock by promoting light-induced degradation of TIMELESS. Science *312*, 1809–1812.

Koike, N., Yoo, S.H., Huang, H.C., Kumar, V., Lee, C., Kim, T.K., and Takahashi, J.S. (2012). Transcriptional architecture and chromatin landscape of the core circadian clock in mammals. Science *338*, 349–354.

Kojima, S., Sher-Chen, E.L., and Green, C.B. (2012). Circadian control of mRNA polyadenylation dynamics regulates rhythmic protein expression. Genes Dev. *26*, 2724–2736.

Kwon, Y.T., and Ciechanover, A. (2017). The Ubiquitin Code in the Ubiquitin-Proteasome System and Autophagy. Trends Biochem. Sci. *42*, 873–886.

Lagarou, A., Mohd-Sarip, A., Moshkin, Y.M., Chalkley, G.E., Bezstarosti, K., Demmers, J.A., and Verrijzer, C.P. (2008). dKDM2 couples histone H2A ubiquitylation to histone H3 demethylation during Polycomb group silencing. Genes Dev. *22*, 2799–2810.

Lamaze, A., Lamouroux, A., Vias, C., Hung, H.C., Weber, F., and Rouyer, F. (2011). The E3 ubiquitin ligase CTRIP controls CLOCK levels and PERIOD oscillations in Drosophila. EMBO Rep. *12*, 549–557.

Le Martelot, G., Canella, D., Symul, L., Migliavacca, E., Gilardi, F., Liechti, R., Martin, O., Harshman, K., Delorenzi, M., Desvergne, B., et al.; CycliX Consortium (2012). Genome-wide RNA polymerase II profiles and RNA accumulation reveal kinetics of transcription and associated epigenetic changes during diurnal cycles. PLoS Biol. *10*, e1001442.

Liu, Y., Singh, S.R., Zeng, X., Zhao, J., and Hou, S.X. (2015). The Nuclear Matrix Protein Megator Regulates Stem Cell Asymmetric Division through the Mitotic Checkpoint Complex in Drosophila Testes. PLoS Genet. *11*, e1005750.

Low, T.Y., Magliozzi, R., Guardavaccaro, D., and Heck, A.J. (2013). Unraveling the ubiquitin-regulated signaling networks by mass spectrometry-based proteomics. Proteomics *13*, 526–537.

Lück, S., Thurley, K., Thaben, P.F., and Westermark, P.O. (2014). Rhythmic degradation explains and unifies circadian transcriptome and proteome data. Cell Rep. *9*, 741–751.

Luo, W., Li, Y., Tang, C.H., Abruzzi, K.C., Rodriguez, J., Pescatore, S., and Rosbash, M. (2012). CLOCK deubiquitylation by USP8 inhibits CLK/CYC transcription in Drosophila. Genes Dev. *26*, 2536–2549.

Martinek, S., Inonog, S., Manoukian, A.S., and Young, M.W. (2001). A role for the segment polarity gene shaggy/GSK-3 in the Drosophila circadian clock. Cell *105*, 769–779.

Martinez, A., Lectez, B., Ramirez, J., Popp, O., Sutherland, J.D., Urbé, S., Dittmar, G., Clague, M.J., and Mayor, U. (2017). Quantitative proteomic analysis of Parkin substrates in Drosophila neurons. Mol. Neurodegener. *12*, 29.

Masri, S., Patel, V.R., Eckel-Mahan, K.L., Peleg, S., Forne, I., Ladurner, A.G., Baldi, P., Imhof, A., and Sassone-Corsi, P. (2013). Circadian acetylome reveals regulation of mitochondrial metabolic pathways. Proc. Natl. Acad. Sci. USA *110*, 3339–3344.

Mauvoisin, D., Wang, J., Jouffe, C., Martin, E., Atger, F., Waridel, P., Quadroni, M., Gachon, F., and Naef, F. (2014). Circadian clock-dependent and -independent rhythmic proteomes implement distinct diurnal functions in mouse liver. Proc. Natl. Acad. Sci. USA *111*, 167–172.

Mauvoisin, D., Dayon, L., Gachon, F., and Kussmann, M. (2015). Proteomics and circadian rhythms: it's all about signaling!. Proteomics *15*, 310–317.

Mendjan, S., Taipale, M., Kind, J., Holz, H., Gebhardt, P., Schelder, M., Vermeulen, M., Buscaino, A., Duncan, K., Mueller, J., et al. (2006). Nuclear pore components are involved in the transcriptional regulation of dosage compensation in Drosophila. Mol. Cell *21*, 811–823.

Menet, J.S., Rodriguez, J., Abruzzi, K.C., and Rosbash, M. (2012). Nascent-Seq reveals novel features of mouse circadian transcriptional regulation. Elife *1*, e00011.

Møller, M., Sparre, T., Bache, N., Roepstorff, P., and Vorum, H. (2007). Proteomic analysis of day-night variations in protein levels in the rat pineal gland. Proteomics *7*, 2009–2018.

Naidoo, N., Song, W., Hunter-Ensor, M., and Sehgal, A. (1999). A role for the proteasome in the light response of the timeless clock protein. Science *285*, 1737–1741.

Neufeld-Cohen, A., Robles, M.S., Aviram, R., Manella, G., Adamovich, Y., Ladeuix, B., Nir, D., Rousso-Noori, L., Kuperman, Y., Golik, M., et al. (2016).

Circadian control of oscillations in mitochondrial rate-limiting enzymes and nutrient utilization by PERIOD proteins. Proc. Natl. Acad. Sci. USA *113*, E1673–E1682.

Ozturk, N., VanVickle-Chavez, S.J., Akileswaran, L., Van Gelder, R.N., and Sancar, A. (2013). Ramshackle (Brwd3) promotes light-induced ubiquitylation of Drosophila Cryptochrome by DDB1-CUL4-ROC1 E3 ligase complex. Proc. Natl. Acad. Sci. USA *110*, 4980–4985.

Peschel, N., Veleri, S., and Stanewsky, R. (2006). Veela defines a molecular link between Cryptochrome and Timeless in the light-input pathway to Drosophila's circadian clock. Proc. Natl. Acad. Sci. USA *103*, 17313–17318.

Peschel, N., Chen, K.F., Szabo, G., and Stanewsky, R. (2009). Light-dependent interactions between the Drosophila circadian clock factors cryptochrome, jetlag, and timeless. Curr. Biol. *19*, 241–247.

Pirone, L., Xolalpa, W., Sigurðsson, J.O., Ramirez, J., Pérez, C., González, M., de Sabando, A.R., Elortza, F., Rodriguez, M.S., Mayor, U., et al. (2017). A comprehensive platform for the analysis of ubiquitin-like protein modifications using in vivo biotinylation. Sci. Rep. *7*, 40756.

Qi, H., Rath, U., Wang, D., Xu, Y.Z., Ding, Y., Zhang, W., Blacketer, M.J., Paddy, M.R., Girton, J., Johansen, J., and Johansen, K.M. (2004). Megator, an essential coiled-coil protein that localizes to the putative spindle matrix during mitosis in Drosophila. Mol. Biol. Cell *15*, 4854–4865.

Ramirez, J., Martinez, A., Lectez, B., Lee, S.Y., Franco, M., Barrio, R., Dittmar, G., and Mayor, U. (2015). Proteomic Analysis of the Ubiquitin Landscape in the Drosophila Embryonic Nervous System and the Adult Photoreceptor Cells. PLoS ONE *10*, e0139083.

Reddy, A.B., Karp, N.A., Maywood, E.S., Sage, E.A., Deery, M., O'Neill, J.S., Wong, G.K., Chesham, J., Odell, M., Lilley, K.S., et al. (2006). Circadian orchestration of the hepatic proteome. Curr. Biol. *16*, 1107–1115.

Robles, M.S., Cox, J., and Mann, M. (2014). In-vivo quantitative proteomics reveals a key contribution of post-transcriptional mechanisms to the circadian regulation of liver metabolism. PLoS Genet. *10*, e1004047.

Robles, M.S., Humphrey, S.J., and Mann, M. (2017). Phosphorylation Is a Central Mechanism for Circadian Control of Metabolism and Physiology. Cell Metab. *25*, 118–127.

Rodriguez, J., Tang, C.H., Khodor, Y.L., Vodala, S., Menet, J.S., and Rosbash, M. (2013). Nascent-Seq analysis of Drosophila cycling gene expression. Proc. Natl. Acad. Sci. USA *110*, E275–E284.

Ruel, L., Pantesco, V., Lutz, Y., Simpson, P., and Bourouis, M. (1993). Functional significance of a family of protein kinases encoded at the shaggy locus in Drosophila. EMBO J. *12*, 1657–1669.

Schilling, B., Rardin, M.J., MacLean, B.X., Zawadzka, A.M., Frewen, B.E., Cusack, M.P., Sorensen, D.J., Bereman, M.S., Jing, E., Wu, C.C., et al. (2012). Platform-independent and label-free quantitation of proteomic data using MS1 extracted ion chromatograms in skyline: application to protein acetylation and phosphorylation. Mol. Cell. Proteomics *11*, 202–214.

Stojkovic, K., Wing, S.S., and Cermakian, N. (2014). A central role for ubiquitination within a circadian clock protein modification code. Front. Mol. Neurosci. *7*, 69.

Tong, L. (2013). Structure and function of biotin-dependent carboxylases. Cell. Mol. Life Sci. *70*, 863–891.

Vaquerizas, J.M., Suyama, R., Kind, J., Miura, K., Luscombe, N.M., and Akhtar, A. (2010). Nuclear pore proteins nup153 and megator define transcriptionally active regions in the Drosophila genome. PLoS Genet. *6*, e1000846.

Wang, J., Mauvoisin, D., Martin, E., Atger, F., Galindo, A.N., Dayon, L., Sizzano, F., Palini, A., Kussmann, M., Waridel, P., et al. (2017). Nuclear Proteomics Uncovers Diurnal Regulatory Landscapes in Mouse Liver. Cell Metab. *25*, 102–117.

Yoo, S.H., Mohawk, J.A., Siepka, S.M., Shan, Y., Huh, S.K., Hong, H.K., Kornblum, I., Kumar, V., Koike, N., Xu, M., et al. (2013). Competing E3 ubiquitin ligases govern circadian periodicity by degradation of CRY in nucleus and cytoplasm. Cell *152*, 1091–1105.

Zhang, Z., Lv, X., Yin, W.C., Zhang, X., Feng, J., Wu, W., Hui, C.C., Zhang, L., and Zhao, Y. (2013). Ter94 ATPase complex targets k11-linked ubiquitinated ci to proteasomes for partial degradation. Dev. Cell *25*, 636–644.

Zimowska, G., Aris, J.P., and Paddy, M.R. (1997). A Drosophila Tpr protein homolog is localized both in the extrachromosomal channel network and to nuclear pore complexes. J. Cell Sci. *110*, 927–944.